DESIGN, CONSTRUCTION AND TESTING OF SOLAR WATER DISTILLATION UNIT FOR RURAL WATER PURIFICATION IN NIGERIA

SAFYANU B. DANJUMA

ABUBAKAR TATARI ALI POLYTECHNIC, BAUCHI. (NIGERIA)

Abstract

This paper presents the design, testing and construction of solar water distillation unit for rural water purification in Nigeria. The construction is done purely with local and affordable materials, for rural dwellers of RafinTambari village of Bauchi, located at Latitude 10.4°N and longitude of 9.5°E. The design consists of twelve stills arrange in two rows of six, with an area of 2m^2 for each solar still attached together. Over-head storage tank of 2000litres capacity for supplying contaminated water from the stream to the solar still, 500litre of storage tank for collecting distilled water and an output device for flushing out waste product out of the solar still. Ambient and operating conditions of the plant are assumed, the same for the twelve solar still. The overall yield at different water depth of 20, 40, 60mm were 5010ml/m^{2}hr, 4465ml/m^{2}hr and 3776ml/m.^{2}hr respectively and the efficiency of the system at different water depth of 20, 40, 60mm were 50.1%, 44.6% and 37.7% respectively. The prevailing operating conditions were: Ambient temperature; 41°C, solar radiation; 1300W/m^2 and wind speed; 3.08m/s. Microbial load analysis of the water before and after distillations were carried out and the following were found: PH of water; 8.2, TDS of water; 100 and 10 mg/l and E.coli; 120 and 20cfu/100ml. The distilled water was certified safe and potable for human consumption

Keywords: Design, Construction, Testing, Water Analysis, Solar Distillation, and Distillate Yield

1. Introduction

Water is the basic necessity for human along with food and air. There is almost no water left on Earth that is safe to drink without purification. Only 1% of Earth's water is in a fresh, liquid state, and nearly all of this is polluted by both diseases and toxic chemicals (Alpesh et al, 2011). For this reason, purification of water supplies is extremely important. Moreover, typical purification systems are easily damaged or compromised by disasters, natural or otherwise. This results in very challenging situations that may cause for such diseases and toxic chemicals to be present in the untreated water. The need to find out the solutions to these problems needs not to be over emphasis. Fortunately there is a solution to these problems. It is a technology that is not only capable of removing a very wide variety of contaminants in just one step, but is simple, cost-effective, and environmentally friendly, that is the use of solar energy.

In addition, there are many locations where stream water is abundant but portable water is not available. Pure water is also useful for batteries and in hospitals or schools.

Green house solar still generally imitates a part of the natural hydrologic cycle in that the Sun's rays heat the saline water so that the production of water vapor (humidification) increases (Chabi, 2000). Horizontal concentric tube solar still utilizes air as working medium. Air carries the water vapor from the annular space between the clear outer and the inner tube through the inside of the inner tube where the water vapor condenses and gives up its heat of condensation directly to the seawater being sprayed on the outer surface of the inner tube. The water vapor will have the preferential tendency to condense on the inside surface of the clear outer tube (Atagunduz, 2001). Cylindrical parabolic type solar still has a parabolic reflector; the reflector is used to concentrate the incident solar radiation on the black outside surface of a tray located on the focal line of the reflector (Minasian et al, 1997).
The aim and objective of this paper is to design, construction and testing of solar water distillation unit for rural water purification and improving the efficiency and productivity of the distilled water.
A solar powered distillation device contain three basic components: a basin in which the contaminated water is contained, a surface above said feed water for the water vapor to condense onto (i.e. a glass pane), and a catch

doi:10.18086/swc.2015.10.45 Available at http://proceedings.ises.org

basin for the distilled water to drain into. During operation of the distiller, solar energy is collected by the feed water. When enough energy is absorbed by the water, the water undergoes a phase change. The water vapors then rises and comes into contact with the cooler transparent, inclined surface. Here the vapor once again goes through a phase change from vapor back to liquid. The water then condenses and runs off the transparent inclined surface into a collection bin. The distillation process rids the contaminated water of any impurities and most commonly found chemical contaminants within the environment. These contaminants are left behind in the basin (Nafey*et al*, 2000). This process is illustrated in Figure 1 below.

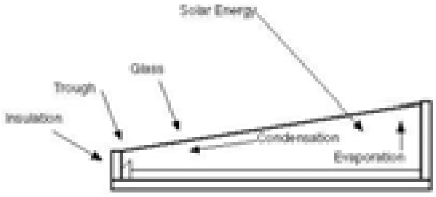

Fig. 1: Basic Solar Powered Water Distiller (Nafey*et al*, 2000).

2.0 Methodology

2.1 Principle of Solar Still Pilot Plant Design and Operation

The solar still pilot plant consists of asymmetrical solar stills arranged in two rows and each of the rows is made of six solar stills, which comprises of total of twelve solar stills. Dimension of $2m^2$, with inclination of 10.4° (base on latitude of Bauchi), orientation of north to south and the same for the entire twelve solar stills.

The solar still consist of three basic components; (a) Basin made of galvanized iron and painted black in which the contaminated water is contained. (b) A glass pane 4mm thickness which covers the solar still and on which vapour condenses. (c) A catch basin, which collects the distilled water into the storage tank (500L).

Each of the stills has an inlet where brackish or contaminated water is fed into the still from the stream via over-head tank (2000L), mark of water depth level of 20mm, 40mm and 60mm and a drain where deposited waste water from the still is flushed after long use. A storage tank (2000L) into which distilled water is pumped from the 500L tank.

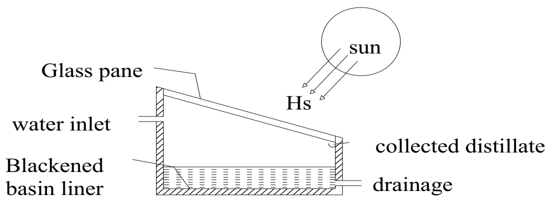

Fig. 2: Conventional solar still (Alkasim, 2012)

3.0 Energy and Mass Balance Method

The performance of a solar still is generally expressed in term of the quantity of water evaporated per unit area of the basin in one day (cubic meters of water per square meter of the basin area per day). This performance of a solar still can be predicted by writing the energy and mass balance equations on the various components of the solar still.

The energy balances for the different components of the solar still are as follows:

3.1 Glass cover

The energy balance for the glass cover can be expressed as follows (Alkasim et al 2012):

$$\tau_1 H_S + [\dot{q}_{rw} + \dot{q}_{cw} + \dot{q}_{ew}] = \dot{q}_{rg} + \dot{q}_{cg} \quad \text{.................................... (eq.1)}$$

H_S – solar radiation on glass cover (W/m^2°C)

$\dot{q}_{rw}$ = internal heat transfer loss by radiation from water surface to the glass

$\dot{q}_{cw}$ = internal heat transfer loss by convention from water surface to the glass

$\dot{q}_{ew}$ = internal heat transfer loss by evaporation

$\dot{q}_{rg}$ = external heat transfer loss by radiation from glass surface to the ambient

$\dot{q}_{cg}$ = external heat transfer loss by convection from glass surface to the ambient

3.2 The Water Content (water mass)

The energy balance for water content inside the solar still is:

$\tau_2 H_S + \dot{q}_w = M_{cw} C_w \frac{dTw}{dt} + \dot{q}_{rw} + \dot{q}_{cw} + \dot{q}_{ew}$ ………………………………. (eq.2)

3.3 The basin liner

The energy balance for the basin liner of the solar still is expressed as

$\tau_3 H_S = \dot{q}_w + \left[\dot{q}_b + \dot{q}_b \left(\frac{A_{ss}}{A}\right)\right]$ ………………………………………………….. (eq.3)

$\dot{q}_w$ = internal heat transfer loss from water
$\dot{q}_b$ = internal heat transfer loss from basin liner
A = still basin area (m^2)
A_{sw} − Side wall area (m^2)

3.4 The Glass Thickness

3.4.1 The External Heat Transfer.

3.4.2 Top loss Coefficient

The glass thickness in most cases is very small. Therefore, the temperature in the glass is assumed uniform. The external heat transfer loss by radiation and convention from the glass cover to ambient, $\dot{q}_g$ can be express as

$\dot{q}_g = \dot{q}_{rg} + \dot{q}_{cg}$ …………………………………………………………….. (eq.4)

$\dot{q}_{rg} = h_{rg}\,(T_g + T_a)$ ………………………………………………………… (eq.5)

Where

$h_{rg} = \frac{\varepsilon_g \sigma[.(T_g + 273)^4 - (T_{sky} + 273)^4]}{(T_g - T_a)}$ ……………………………………………….. (eq.6)

And

$\dot{q}_{cg} = h_{cg}(T_g - T_a)$..…………………………………………………………… (eq.7)

Substituting equations (eq.5) and (eq.7) into equation (eq.4), we get

$\dot{q}_g = h_1(T_g - T_a)$……………………………………………………………….. (eq.8)

Where

$h_1 = h_{rg} + h_{cg}$ ……………………………………………………………….. (.eq.9)

$h_1$is expressed empirically to include the effect of free convection and radiation from the glass cover (Ilaria et al, 2010). The expression is;

$h_1 = 5.7 + 3.8V \qquad 0 \leq V \leq 5ms^{-1}$ ………………………………………. (eq.10)

Where V is the wind speed measured in ms^{-1}. The expression for a zero wind speed gives heat loss by natural convection.

3.4.3 Bottom and side loss coefficient

The heat loss from the water in the solar still to the ambient through the thick insulation (sawdust) and subsequently by convection and radiation from the bottom, and sides surfaces of the basin, can be written respectively as

$U_b = \left[\frac{1}{h_w} + \frac{1}{h_b}\right]^{-1} = \left[\frac{1}{h_w} + \frac{1}{\frac{K_i}{L_i}} + \frac{1}{h_{cb+}h_{rb}}\right]^{-1}$ …………………………………… (eq.11)

$U_{sw} = U_b F_1 = \left[\frac{1}{h_w} + \frac{1}{\frac{K_i}{L_i}} + \frac{1}{h_{cb+}h_{rb}}\right]^{-1} \left(\frac{A_{ss}}{A}\right)$……………………………………… (eq.12)

The rate of heat loss from the basin liner to the ambient per m^2 can be written as;

$\dot{q}_b = h_b(T_b - T_a)$ ……………………………………………………………...(eq.13)

Where

$h_b = \left[\frac{L_i}{K_i} + \frac{1}{h_{cb} + h_{rb}}\right]^{-1}$ ………………………………………………………… (eq.14)

3.4.4 The internal heat transfer

3.4.5RadiativeLoss Coefficient

The rate of heat transfer, $\dot{q}_{rw}$from the water surface to the glass for infinite parallel plane is given by (Tiwari 2004, Garba and Maduekwe, 1996 and Alkasim et al, 2012)

$\dot{q}_{rw} = h_{rw}(T_w - T_g)$……………………………………………………… …. (eq.15)

Where h_{rw} is given by

$$h_{rw} = \sigma \left[\frac{(T_w+273)^2+(T_w+273)^2}{\left(\frac{1}{\varepsilon_w}+\frac{1}{\varepsilon_w}\right)^{-1}}\right](T_w + T_g + 546) \quad \text{(eq.16)}$$

With

$$\varepsilon_{eff} = \left(\frac{1}{\varepsilon_w} + \frac{1}{\varepsilon_w} - 1\right)^{-1} \quad \text{(eq.17)}$$

3.4.6Convective Loss Coefficient

There is heat transfer across the humid air inside the distiller unit by free convection, which is caused by the effect of buoyancy, due to density variation in the humid fluid, which occurs due to the temperature gradient in this fluid. The rate of heat transfer from the water surface to the glass cover, $\dot{q}_{cw}$by convection in the upward direction through the humid fluid can be estimated as

$$\dot{q}_{cw} = h_{cw}(T_w - T_g) \quad \text{(eq.18)}$$

The internal convective heat transfer coefficient, h_{cw}, from heat flow from the horizontal basin (hottest region in the still) to the water mass in the basin and vice-versa is determined from the following relations (Sodar et al, 1980, Egarievwe 1989, Tiwari, 2004, Saini and Saini, 2008 and Alkasim, et al 2012)

$$Nu = Co\,(Gr.\,Pr)^{no} \quad \text{(eq.19)}$$

Where

$$Nu = \frac{h_{cw} X_1}{K_w} \quad \text{(eq.20)}$$

$$Gr = \frac{X_1^3 \rho_{wg\beta\Delta T}^2}{\mu_w^2} \quad \text{(eq.21)}$$

$$Pr = \frac{C_{pw}\mu_w}{k_w} \quad \text{(eq.22)}$$

$$\Delta T' = \left[\Delta T + \frac{(P_w - P_g)(T_w - 273)}{0.2689 - P_w}\right] \quad \text{(eq.23)}$$

$$\Delta T = T_w - T_g \quad \text{(eq.24)}$$

And for normal operating temperature range, say 45°C $\Delta' T$ = 17°C, expression for Gr reduces to (Tiwari, 2004)

$$Gr = 2.81 \times 10 X_1^3 \quad \text{(eq.25)}$$

Table 1: values of Grashofnumber, Gr
for various average spacing X_1

X1(m)	Gr	Co	no
0.15	0.948×	0.21	¼
0.2	10^5	0.21	¼
0.25	2.248×	0.075	⅓
	10^5		
	4.390×		

Source: (Tiwari, 2004)

As it can be seen from equation (eq.25) (Gr) depends on X_1 (Table 1). This Table gives the value of Gr for different X_1.

The value of *Pr* remains constant and, as given by equation (eq.22). For the normal operating temperature range and at spacing, X_1 = 0.25m; the value of the constant *Co* is: - *Co* = 0.075 and $n_o = \frac{1}{3}$. After substituting for the expressions of *Nu,* Gr and *Pr* in equation (eq.19), the convective heat transfer coefficient h_{cw} becomes

$$h_{cw} = \frac{C_o K_w}{X_1} \cdot \left[\frac{X_1^3 \rho_{wg\beta\Delta T}^2}{\mu_w^2} \cdot \frac{C_{pw}\mu_w}{k_w}\right]^{1/3} \quad \text{(eq.26)}$$

Dunkle, (1991) also derived the following expression for h_{cw} as thus:

$$h_{cw} = 0.884\left[T_w - T_{g+}\frac{(P_w - P_g)(T_w + 273)}{0.2689 - P_w}\right]^{1/3} \quad \text{(.eq.27)}$$

3.4.7Evaporative Heat Loss Coefficient

The mass transfer coefficient, h_e , in terms of convective heat transfer coefficient h_{cw} , the total gas pressure, P_T, the mass of the water vapour, M_w, the air mass, M_a, the specific latent heat, L, and specific heat per unit volume at constant pressure, C_{pa} of the mixture is given by (Alkasim et al, 2012) as

$$\frac{h_e}{h_{cw}} = \frac{L}{C_{pa}}\left(\frac{M_w}{M_a}\right)\left(\frac{1}{P_T}\right) \quad \text{(eq.28)}$$

The expression in (eq.28) is formulated owing to the assumption that;

(i) The exchange of the water vapour with the boundary layers at both the water and glass surfaces is neglected and (ii) P_w & $P_g$are considered small compared to P_T.

The rate of heat transfer per unit area from the water surface to the glass cover is obtained by substituting the appropriate values for the parameters in equation (eq.28) thus;

$$\dot{q}_{ew} = 0.013 h_{ew}(P_w - P_g) \quad \text{(eq.29)}$$

$$\dot{q}_{ew} = h_{ew}(T_w - T_g) \quad \text{(eq.30)}$$

From (eq.29) and (eq.30) we can write h_{ew} as

$$h_{ew}=1.6273\times10^{-4} h_{cw}\left(\frac{P_w-P_g}{T_w-T_g}\right) \quad \text{(eq.31)}$$

It is important to mention here that the value of h_{ew} can be more realistic for larger value of$(T_w - T_g)$. The values of P_W and P_g (for the range of temperature 10°C - 90°C) can be obtained from the expression (Fernandez and Chargoy, 1990).

$$P_T = \exp\left[25.317 - \frac{5144}{(T-273)}\right] \quad \text{(eqn.32)}$$

The total internal heat transfer coefficient $h_2$is the sum of the three internal heat transfer coefficient which can be written as:

$$h_2=\left[\frac{(T_w+273)^2-(T_g+273)}{\left(\frac{1}{\varepsilon_w}+\frac{1}{\varepsilon_g}-1\right)}\right](T_w + T_g + 546)+0.884\left[T_w + T_g + \frac{(P_w+P_g)+(T_{w+273})}{268.9\times10P_w}\right]^{1/3} + 16.273\times10^{-3} + 16.273\times10^{-3}h_{cw}\frac{P_w-P_g}{T_w-T_g}$$

4.0 Results and Discussion

In this section, average hourly solar radiation, temperature difference of ambient and still conditions and also average hourly and overall distillate yield of the solar still at water depth of 20, 40, and 60mm respectively was observed and recorded, to evaluate the design, construction and testing of the solar distillation pilot plant rural water supply.

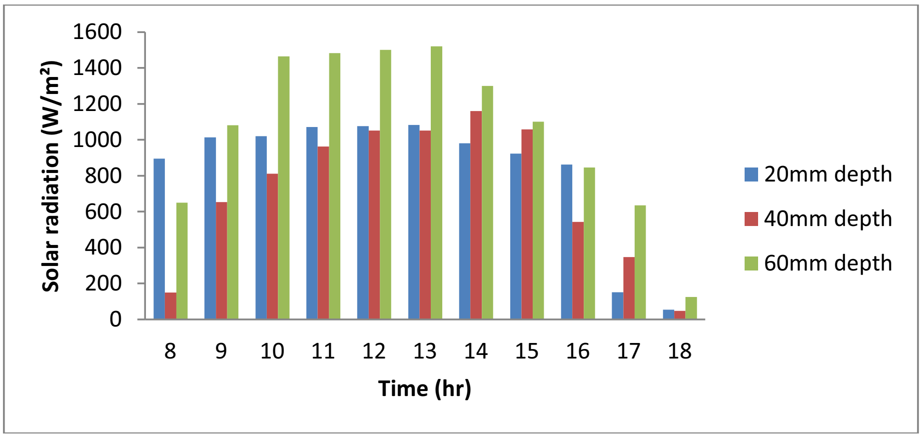

Fig.3: Average Hourly Solar Radiations

Figure 3 depicts Average hourly solar radiation at different water depth of 20, 40, and 60mm which shows highest solar radiation was recorded between 12noon to 13pm.

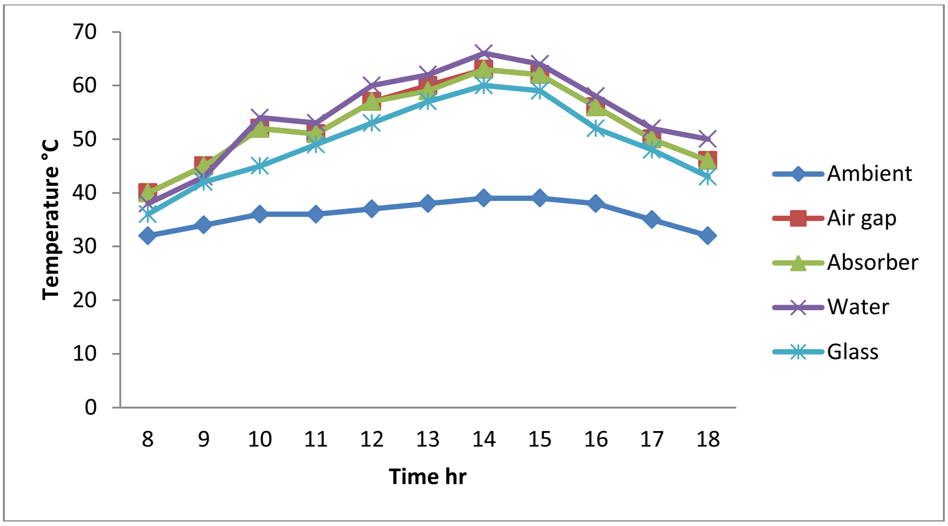

Fig. 4: Average Hourly Temperatures of Ambient and still conditions (20mm depth)

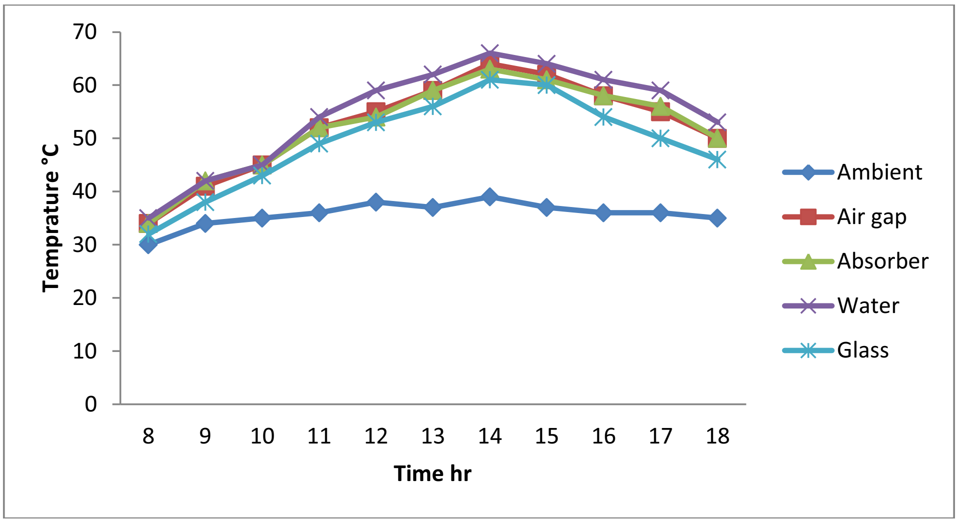

Fig.5: Average Temperature differences of Ambient and still conditions (40mm depth)

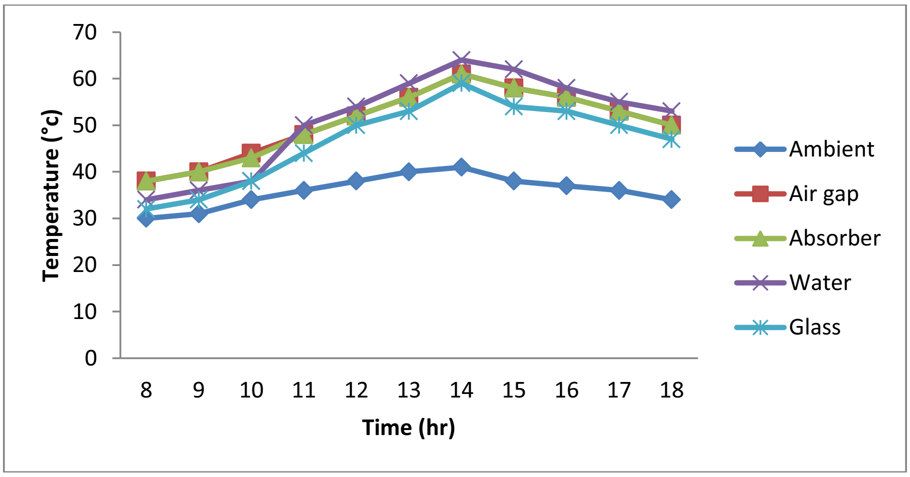

Fig.6:Average Temperature differences of Ambient and still conditions (60mm depth)

Figures (4, 5 and 6) depict Hourly temperature difference of ambient and still conditions at water depth of 20, 40 and 60mm. After observation it shows that the temperature increases with time in ascending order of highest ambient, highest glass, highest air-gap, highest water and highest absorber plate temperatures. This confirmed that the solar radiation energy is directly absorbed by the absorber plate due to high thermal conductivity as heat, which is transfer to the water, then change of state takes place from liquid to vapor as the water evaporate within the air-gap, it increases the temperature of the air-gap. As vapor makes contact with glass cover it condenses due to decrease in temperature difference. Condensations take place because the temperature of the air-gap is greater than the glass temperature and the ambient is lower than the glass temperature (Robert *et al,* 2010)

Table 1: Average Overall Hourly Distillate Yield

Time (hr)	**Yield(ml/m²hr) 20mm depth**	**Yield(ml/m²hr) 40mm depth**	**Yield(ml/m²hr) 60mm depth**
8-9	10	8	4
9-10	17	15	11
10-11	68	60	45
11-12	160	154	123
12-13	342	256	198
13-14	403	389	287
14-15	560	423	396
15-16	602	589	476
16-17	654	603	501
17-18	680	620	512
18-19	701	625	522
19-7	813	723	701

Table 1 shows the average hourly distillate yield. It is obvious that yield of a still is affected by the water depth. The lower the water depth the greater the yield, 20mm water depth yield distillate of 5100ml/m^2.hr and the higher the water depth the lower the yield, 60mm water depth yield distillate of 3776ml/m2.hr

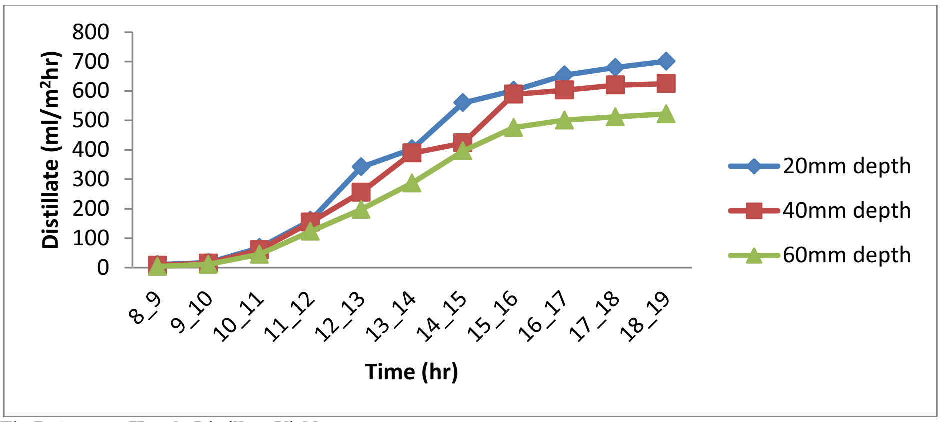

Fig.7: Average Hourly Distillate Yield

Figure 7 shows the hourly distillate yield at 20mm water depth, yield the highest distillate with time and 60mm water depth, yield the lowest distillate with time. Efficiency of the still was also affected by water depth, 20mm water depth with efficiency of 50.1%, 40mm water depth with efficiency of 44.6% and 60mm water depth with efficiency of 37.7%. The efficiency was used to evaluate the performance of the still. (Buros, 20000)

5.0 Conclusion

The design, construction and testing of solar distillation pilot plant was evaluated with water depth was set at 20, 40, and 60mm respectively. Average hourly solar radiation at different water depth mention above, which shows that highest solar radiation was recorded between 12noon to 1pm. Hourly temperature difference of ambient and still conditions were observed which shows that the temperature increases with time in ascending order of highest ambient, glass, air-gap, water, and absorber plate temperatures. Also the average hourly distillate yield was recorded and it is obvious the yield of the still is affected by water depth. Overall yield of distillate were found to be 60.12litre at 20mm water depth, 53.58litre at 40mm water depth and 45.31litres at 60mm respectively and efficiency of the system at different water depth of (20, 40, 60mm) were found to be 50.1%, 44.6% and 37.7% respectively.

Nomenclature

A - Still basin area (m^2)

A_g - Glass covers area (m^2)

A_s - Total still area (m^2)

A_{sw} − Side wall area (m^2)

B - Breadth of still (m)

C_w - Specific heat of water (J/kg°C)

F_1 - Glass area correction factor (A_s/A)

L - Length of still (m)

g -Acceleration due to gravity (m/s^2)

h_1 − Radiative heat transfer coefficient from water to glass cover (W/m^2°C)

h_2 - Convective heat transfer coefficient from glass cover to ambient (W/m^2°C)

h_3 - Heat transfer coefficient from water to the basin liner (W/m^2°C)

h_{rw} - Radiative heat transfer coefficient (W/m^2°C)

h_{cw} --Convective heat transfer coefficient (W/m^2°C)

h_{ew} - Evaproative heat transfer coefficient (W/m^2°C)

H_s - Solar radiations on the glass cover (W/m^2)

k_w - Thermal conductivity of the water in the basin (W/m^2)

ℓ - Water depth in the basin (m)

m - Distilled water production rate (kg/min)

m_t - Total distilled water production (kg)

M_w - Water content in the basin (kg)

Gr – Grashof number

Nu – Nusselt number

Pr - Prandtl number

P_g - Water vapour pressure at glass temperature (Pa)

P_w - Water vapour pressure at water temperature (Pa)

Q_{ew} - Mass of evaporated water (kg)

$\dot{q}$ - Rate of energy transfer (J/s)

R_b - Basin liner reflectivity

R_g - Glass cover reflectivity

R_w - Water surface reflectivity

R.H. - Relative humidity (%)

t - Time (s)

T_a - Ambient temperature (°C)

T_b - Basin liner temperature (°C)

T_g - Glass temperature (°C)

T_w - Water temperature (°C)

U_T - Top loss coefficient (W/m^2°C)

U_B - Bottom loss coefficient (W/m^2°C)

U_{sw} - Overall heat transfer coefficient from the side wall to the ambient (W/m^2°C)

V - The wind velocity (m/s)

X_1 - Water to glass spacing (m)

Reference

AlkasimAbubakar, AdamuUsman and Ododo, J.C., (2012); A Theoretical Solar Distiller Model for Yola North-Eastern, Nigeria, Nigeria Journal for Solar Energy Vol. 23 Pp, 77- 88

Alpesh Mehta, ArjunVyas, NitinBodar, DharmeshLathiya, (2011); Design of Solar Distillation Systems. Vol.29, Pp 11 – 19.

Atagunduz, G., (2001); Solar Desalination, Ege University.

Buros , O.K., (2000); The ABC's of Desalting, TopfiedMassachusett, USA.

Chabi, M.T., (2000); An Overview of Solar Desalination for Domestic and Agriculture Water needs in Remote Arid Areas, Desalination **127**, Pp.119 – 133

Egarievwe, S.U., (1989); Solar Still for Fresh Water Production in Rural Areas- Design and Economic Consideration, Nigerian Journal of Energy, **8**(8).

Fernandez, J. and Chargoy, N. (1990), Multistage, Indirectly Heated Solar Still, Solar Energy, **4** (44): Pp. 215.

Garba, A.T. and Maduekwe, (1996); Mathematical Modelling of Some Renewable Energy Systems: A case study of Solar Cooker, Solar Still, Solar Water Heater, Saw dust and Improved Wood- Burning Stoves, Nigeria Journal of Renewable Energy, Vol. 4 (2), Pp. 1 – 11.

Ilaria B., Francesco, c., Marco, C., Matteo De, F., Biaggio Di, P., Francesca, M., Stefano, P., Giovanni, P. (2010), Ambient Temperature Modelling with Soft Computing Techniques, Solar Energy, **84:** Pp. 1264-1272.

Minasian, A.N., Al-Karaghouli, A.A. and Habeeb,S.K., (1997); Utilization of aCylindrical Parabolic Reflector for Desalination of Saline Water, Energy Conversion and Management **38** Pp 701 – 704.

Nafey, A.S., Abdelkader, M., Abdelmotalip, A.A. and Mabrouk, A.A., (2000); Parameter Affecting Solar Still Productivity, Energy Conversion and Management (41) 1797

Robert Foster, MajidGhasseni, and Alma Cota, (2010); Solar Energy (Renewable Energy and the Environment), Taylor and Francis, USA.

Saini, S.K., and Saini, R.P., (2008), Development Of Correlation For Nusselt Number And Friction Factor Solar Air-Heater With Roughened Duct Haring Arc-Shaped Wire As Artificial Roughness, Solar Energy **82** Pp 1118 – 11130.

Sodar, M.S., Nyak, J.K., Tiwari, G.N. and Kumar, A., (1980); Double Basin Water Still Energy Conversion **20** (1) m 23

Tiwari , G.N., (2004); Solar Energy Fundamentals, Design, Modelling Applications, 2nd Edition, Narosa publishing house Mumbai.